01,19

Thermal properties of Ti$_3$Al and Zr$_3$Al intermetallides with L1$_2$ superstructure. Molecular dynamics method

© E.B. Dolgusheva

Udmurt Federal Research Center, Ural Branch Russian Academy of Sciences,
Izhevsk, Russia

E-mail: elena@udman.ru

Within the framework of the molecular dynamics method with multiparticle interatomic interaction potentials, studies of the thermodynamic properties of ordered intermetallides Ti$_3$Al, Zr$_3$Al with a structure of type L1$_2$ have been carried out. The results of calculations of the vibrational spectra and thermal properties of intermetallides are compared with the data obtained from the first principles based on the density functional theory. The results of calculations by both methods show that the spectra of compounds are similar in morphology and have intervals of forbidden frequency values. The temperature dependences of the lattice thermal conductivity coefficients Ti$_3$Al and Zr$_3$Al are obtained using the method of nonequilibrium molecular dynamics. On the thermal conductivity graph in a system with zirconium, „plateaus" are observed in the temperature range $200\,\mathrm{K} < T < 300\,\mathrm{K}$, where the values of thermal conductivity practically do not change.

Keywords: molecular dynamics method, vibrational densities of states, lattice heat capacity, lattice thermal conductivity.

1. Introduction

Recently, much attention was paid to the study of the thermal properties of non-metals and semiconductors due to the demand for this knowledge in the creation of various technical devices, the main functions of which are performed using thermal regulation [1–3]. However, the correct theoretical description of the temperature dependence of lattice thermal conductivity in metals is yet absent. Strict *ab initio* calculations are usually limited to zero temperature [4], and parameters are introduced to take temperature into account. Molecular dynamics facilitates the study of temperature-dependent properties. In determining such thermal properties of the lattice as thermal conductivity, heat capacity, thermal expansion, etc., atomic vibrations play an important role. The properties of materials whose vibrational spectra contain a frequency range with zero contribution — „gap" are of particular interest. These compounds include intermetallides Ti$_3$Al, Zr$_3$Al with structure of L1$_2$ type.

Structured intermetallides Ti$_3$Al, Zr$_3$Al are „chain-type" crystals in which Zr(Ti) and Al atoms alternate in a face-centered cubic (FCC) lattice, Moreover, the mass of the Zr atom by ~ 3.4 times, and of Ti atom by 1.8 times exceed mass of Al. The presence of „chain" structure, with a significant difference in atomic masses, leads to the appearance of „gap" in the vibrational spectrum of these compounds. The compound Zr$_3$Al has properties (high-temperature strength, corrosion resistance and low thermal neutron absorption) that make it promising for its use in various high-tech areas of industry and nuclear energy. Ti$_3$Al

intermetallide with L1$_2$ superstructure does not exist in the phase diagram. This phase is considered metastable; however, it was discovered experimentally during rapid cooling and subsequent annealing of γ-TiAl phase [5]. Note that the FCC phase for pure zirconium and titanium is also metastable and is observed experimentally in film samples only [6–8]. Metastable materials may have physical properties that differ from the properties of the equilibrium state, since a different set of vibrational modes is realized in them. This adds interest to the study of such system properties.

In our early papers [9–11], using the molecular dynamics (MD) method we studied various dynamic and thermal properties of both pure FCC Zr, Ti and Al, and their various systems in the bulk and film states. In particular, the vibrational densities of states of the lattice of intermetallides Ti$_3$Al and Zr$_3$Al, obtained in the paper [11], showed that in both cases the vibrational spectra have „gap". In papers [12,13] the temperature dependences of the lattice thermal conductivity coefficients of pure FCC-Al, -Zr and -Ti were calculated. Moreover, the obtained temperature dependence of the lattice thermal conductivity of FCC-Al is consistent with the results of *ab initio* calculations taking into account phonon-phonon scattering.

In this paper, within the framework of MD method with multiparticle interatomic interaction potentials, calculations of the thermal characteristics of compounds Ti$_3$Al and Zr$_3$Al with superstructure of type L1$_2$ were carried out. The resulting total and partial phonon spectra, as well as the thermal capacity of both compounds, are compared with *ab initio* calculations. The temperature dependences of the

Elastic properties of intermetallides Ti_3Al and Zr_3Al. Equilibrium lattice constant a_0 (Å), bulk modulus B, shear modulus C' and elastic moduli C (GPa)

	Method	a_0	B	C'	C_{11}	C_{12}	C_{44}	Source
Ti_3Al	DFT(GGA)	4.046	112.157	26.08	146.936	94.767	88.432	[20]
	MD	4.09	118.2	34.16	165.8	97.4	51.2	[11]
Zr_3Al	DFT(GGA)	4.375	98.706	25.87	132.155	81.981	70.586	[21]
	DFT(LDA)	3.951	80.8	−	−	−	−	[22]
	MD	4.34	93.5	19.6	119.7	78.43	46.5	[11]

lattice thermal conductivity coefficients of Ti_3Al and Zr_3Al compounds were calculated.

2. Details of calculation of phonon spectra and thermal capacities of Ti_3Al and Zr_3Al

To describe the interatomic interaction multiparticle potentials were used, made within the framepaper of „embedded atom" model (EAM) [14]. For the system Zr_3Al the potentials are taken from [15], and for Ti_3Al from [16]. In these papers it was shown that potentials make it possible to obtain, with a high degree of accuracy, lattice constants, cohesive energies, elastic constants, melting temperatures and other physical characteristics of both pure Zr, Ti and Al, and their various compounds. Previously, with these potentials in paper [11] we calculated lattice constants, elastic moduli, phonon spectra, and heat capacities for pure FCC-Zr, -Ti, -Al, as well as their various Zr/Ti-Al systems. Since all methods for calculating the listed physical variables are described in detail in [11]. Here we only note that the obtained values of lattice constants and elastic moduli for FCC-Zr and -Ti are consistent with those calculated *ab initio* and observed in experiments when producing films of these metals. The lattice constant of Zr_3Al structure in experiments [17–19] is in the range — of 4.29 to 4.392 Å in our calculations $a_0 = 4.34$ Å, which is quite satisfactory. Ti_3Al lattice constant obtained in the experiment [5] is $a_0 = 3.994$ Å, in MD calculations — 4.09 Å.

Figure 1, a, b shows total and partial vibrational densities of states for Ti_3Al (a) and Zr_3Al (b) with superstructure of type $L1_2$. The spectra were obtained on the basis of MD calculations, using the fast Fourier transform of autocorrelation functions of rates averaged over the time interval ~ 30 ps. Calculations were made at temperature $T = 100$ K. From the data presented in Figure 1, a, b it is clear that the spectra are similar in morphology, since both compounds have the same type of structure. In both cases, the low-frequency region contains clearly visible four main peaks, and it almost in full is due to vibrations of the heavier titanium or zirconium atoms. In the high-frequency region the states are determined mainly by vibrations of light

aluminum atoms. In titanium compound the partial contributions of titanium atoms to the high-frequency region, and of aluminum atoms to the low-frequency region are somewhat larger than the corresponding contributions in the compound with zirconium. In Zr_3Al the cutoff frequency is much lower than in Ti_3Al. This is a consequence of the mass ratio, since zirconium is by more than 2 times heavier than titanium. Accordingly, the band gap in the system with zirconium is lower in frequency, besides, it is much wider than in Ti_3Al. In Zr_3Al the band gap has a width of several tens of degrees ($\sim 280-360$ K), and in Ti_3Al — only few degrees ($434-441$ K).

The same Figure 1, c, d, e shows the total and partial spectra Ti_3Al [20], Zr_3 Al [21], Zr_3 Al [22] obtained *ab initio*. In both cases of *ab initio* calculations a method based on density functional theory (DFT) was used. In papers [20,21] the exchange-correlation interaction function is calculated in the generalized gradient approximation (GGA), and in [22] — in the local density approximation (LDA). Note that the graphs presented in the paper [22] with the results of calculations of phonon dispersion and vibrational density of states (see Figure 2 in [22]) show wrong units of measurement: instead cm^{-1} — THz. It is clear that this is unfortunate misprint, since the authors compare their results with the results obtained in the paper [21], where the calculation results of the phonon spectra are given in cm^{-1}. For easy comparison the original frequency scales THz (Figure 1, c) and cm^{-1} (Figure 1, d, e) were converted to temperature units in all graphs. From the comparison of the results obtained by different methods, it is clear that the cutoff frequencies of the spectra of both compounds in MD calculations are higher than in *ab initio* calculations. This is especially strongly observed for Ti_3Al system, although all spectra are similar in morphology. As can be seen from Figure 1, c, d, e, the vibration spectra of atoms Ti_3Al and Zr_3Al, obtained by *ab initio* methods also have bands of prohibited values. However, if in Ti_3Al the width of „gap" is comparable in calculations by both methods, then in the system with zirconium MD and DFT calculations in the LDA approximation give width of „gap" by about $2-2.5$ times greater than the calculation carried out in GGA approximation.
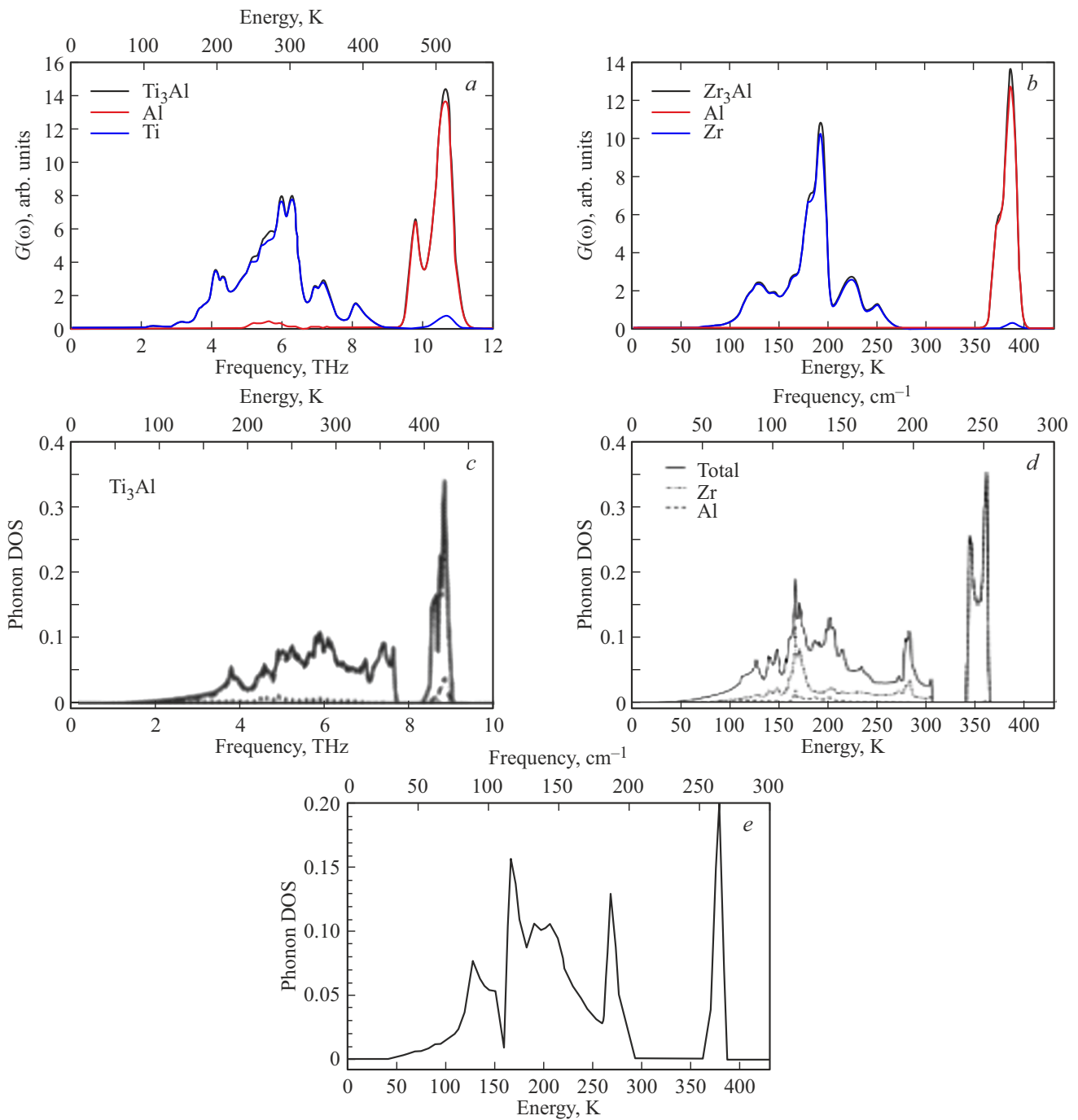
Figure 1. Total and partial vibrational densities of states (VDOS) of compounds with structure of type $L1_2$ obtained using MD method: a — Ti₃Al, b — Zr₃Al; calculated *ab initio*: c — Ti₃Al [20], d, e — Zr₃Al, [21,22] respectively.

For comparison, the Table shows the elastic moduli of intermetallides Ti₃Al and Zr₃Al with cubic structure of type $L1_2$ obtained using molecular dynamics and *ab initio*.

The Table shows that in the system with titanium, the lattice constant and all elastic moduli in the MD method are slightly higher than in DFT calculation. In combination with zirconium, on the contrary, the lattice constant and the values of all moduli are lower than the corresponding values obtained *ab initio*.

Figure 2 shows heat capacities vs. temperature: (a) — Ti₃Al, (b) — Zr₃Al. Dark solid lines show results obtained by *ab initio* methods taken from [20] and [21] respectively. The colored lines indicate the heat capacities calculated using the vibrational spectra from MD calculation. As can be seen from the graphs comparison, in the temperature range $100-300$ K MD calculations give a slightly underestimated value of the heat capacity compared to the results obtained by *ab initio* methods. Moreover, in
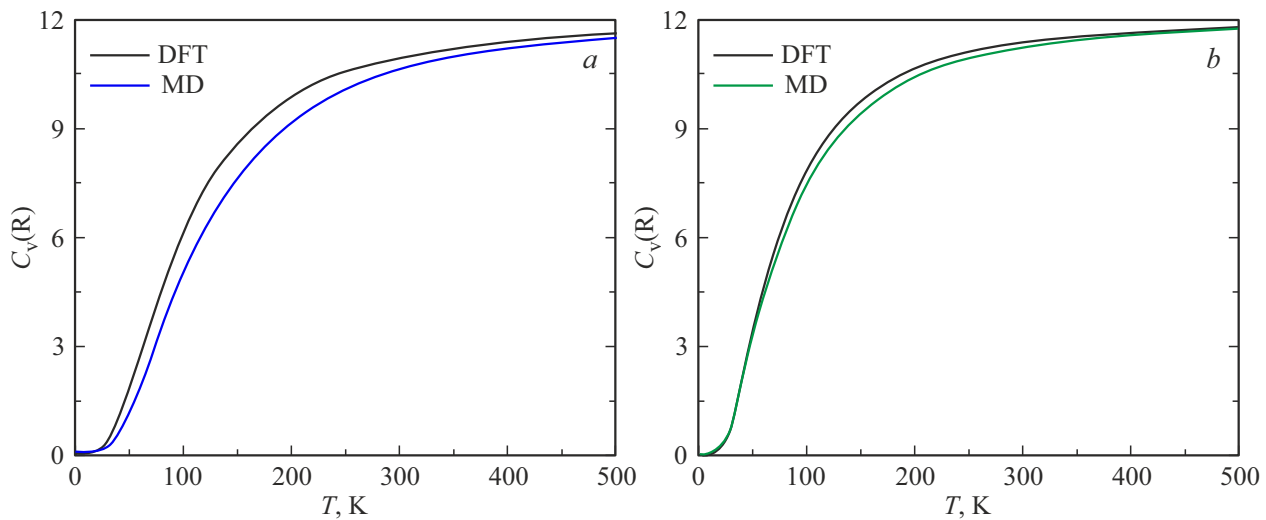
Figure 2. Heat capacity vs. temperature $C_v(R)$ of compounds with lattice type $L1_2$: a — Ti_3Al, it b — Zr_3Al. Dark lines — *ab initio* calculations from [20] and [21], respectively; colored lines — MD calculations.

the system with titanium, this difference is much more noticeable, which is explained by the different distribution of vibrational energy contributions for different methods of phonon spectra calculation.

3. Scheme for lattice thermal conductivity calculation

MD calculations of thermal conductivity were performed using the LAMMPS package [23], which is widely used for molecular and atomic simulations. To calculate the lattice thermal conductivity coefficient, the „eHEX" algorithm, built into the LAMMPS package [24], was used based on the non-equilibrium molecular dynamics method (NEMD) [25]. The NEMD method has direct and reverse options. In reverse option — the heat flow is imposed on the system, and the temperature gradient is obtained as a result of the modeling. Just this option was used in calculations on base crystallites with cross section 12×12 (x, y) and 48 and 96 lattice cells (u.c.) long along the axis z, which corresponds to approximately $5 \times 5 \times 20$ and $5 \times 5 \times 40$ nm. Cyclic boundary conditions were specified along all axes. The crystallites relaxation at a given temperature was carried out for 2 ns. After that, zones with „hot" and „cold" thermostats were set by adding and removing the same portion of energy at each time step. The heat flow was formed between the thermostats along the axis z. The attainment of a stationary heat flow mode at given temperature was simulated for 3 ns. To obtain the temperature profile, the entire crystallite was divided into layers, perpendicular to the heat flow, one lattice cell thick. The kinetic energy of atoms in each layer was averaged over a time interval of 2 ns, after the stationary flow was established. The values of the lattice thermal conductivity coefficient (k_p) were calculated

according to the scheme proposed in [26]:

$$dQ/dt = -k_p \cdot S \cdot \Delta T / \Delta Z.$$

Here dQ/dt — energy flow per unit time ($dt = 1$ fs), S — time-averaged crystallite cross section, $\Delta T / \Delta Z$ — temperature gradient taken on a *linear* section of the temperature profile and averaged over time. Of all the variables the only input parameter is the amount of energy dQ, and all the rest are obtained as a result of the modeling.

In the paper [12], using this algorithm, and taking into account the linear region of the temperature profile only, we obtained the temperature dependence of the lattice thermal conductivity of FCC-Al, which is consistent with the results of *ab initio* calculations performed based on the density functional theory, and taking into account the phonon-phonon interaction only. All features of this scheme use for calculating the phonon thermal conductivity of metals are also described in detail there.

Thus, based on the results of calculations of aluminum thermal conductivity, it became possible to use this approach to calculate the lattice thermal conductivity of metal compounds. Previously such method was used to obtain the temperature dependences of the lattice thermal conductivity coefficients for FCC-Zr and -Ti [13].

4. Lattice thermal conductivity of intermetallides Ti_3Al and Zr_3Al

According to described scheme the gemperature dependences of lattice thermal conductivity for Ti_3Al and Zr_3Al with structure of type $L1_2$ were calculated. At each *set* temperature value several calculations k_p (below 300 K — 5, above — 3) were performed to determine the relative error. The results of calculations are presented in Figure 3. Figure 3, a shows that the behavior of lattice thermal
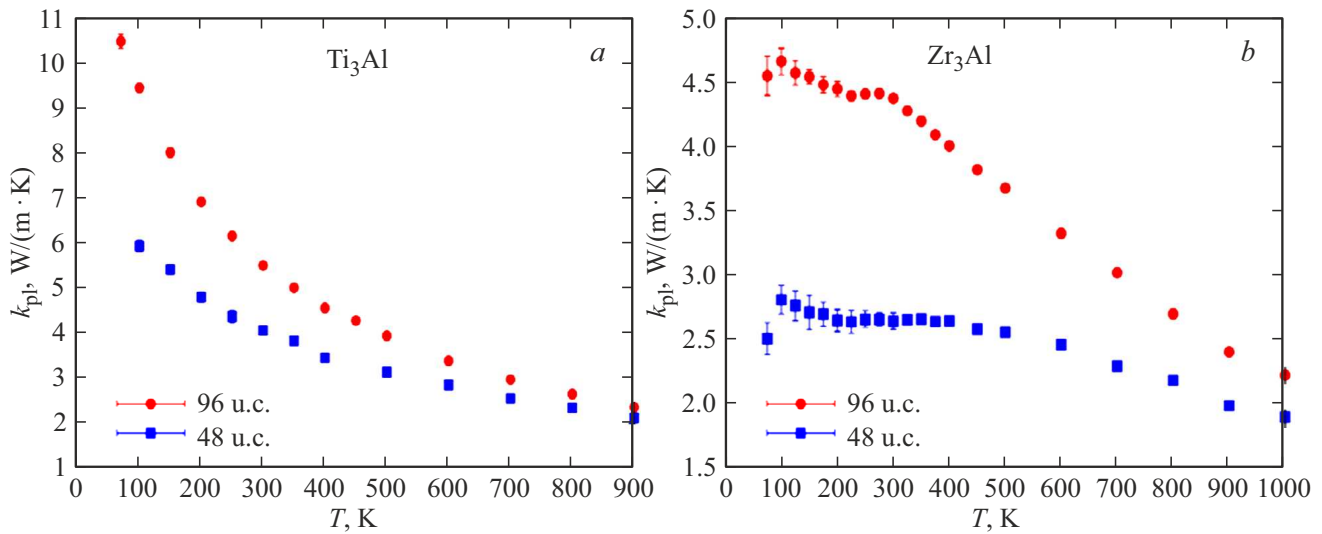
Figure 3. Lattice thermal conductivity vs. temperature $k_p(T)$: (a) — Ti$_3$Al; (b) — Zr$_3$Al. Circles indicate values k_p obtained for crystallites 96 u.c. long, and squares — 48 u.c. long

conductivity of Ti$_3$Al is usual, it decreases with temperature increasing. Crystallites with a longer length (96 u.c.) have a higher thermal conductivity compared to crystallites 48 u.c. long. Since at low temperatures the main contribution to the thermal conductivity coefficient is provided by long-wave phonons, and there number in crystallite with length of 48 cells is lower than in sample with length of 96 cells. With temperature increasing, the difference in values k_p for crystallites of different sizes decreases. As can be seen from the graph in Figure 3, b, the temperature dependence of the thermal conductivity of Zr$_3$Al has abnormal behavior: for a sample 96 u.c. long in the temperature range 200–300 K, and for crystallite 48 u.c. long an even longer „plateau" — from 200 to 400 K is observed.

One can assume different options explaining this behavior of the temperature dependence $k_p(T)$ in Zr$_3$ Al: one — this is a manifestation of the abnormal nature of the lattice thermal conductivity curve in pure FCC Zr, as shown in [13] the peak on the graph $k_p(T)$ is in the region of rather high temperature — 300 K (possibly due to the strong anharmonicity of the potential); another option — this may be due to the presence of a rather wide „band gap" in the spectral density of vibrations, which exists up to 450 K. In this compound the optical and acoustic modes, which are mainly responsible for thermal conductivity, are clearly separated along the aluminum and zirconium sublattices. Besides, the positions of their main peaks on the vibrational density curve differ by exactly two times (192 and 384 K). Although it is believed that optical phonons are not very efficient in transferring energy, they can, however, interact with acoustic ones and thereby affect the heat flow.

Calculations of the vibrational densities of Ti$_3$Al and Zr$_3$Al showed that with increase in temperature the spectra in both compounds „soften", and the „gap" width decreases.

Figure 4 shows the total vibrational densities of both compounds in the region of „gap" at different temperatures: (a) — Ti$_3$Al, (b) — Zr$_3$Al. As can be seen from these graphs, in the system Ti$_3$Al at $T = 200$ K the band gap practically disappears — „collapses", i.e. In the region of these energies vibrations arise that will contribute to phonon-phonon scattering. Whereas, in Zr$_3$Al system the band gap is maintained up to $T = 400$ K, inclusive, only its width decreases. At $T = 75$ K is about 70 K, and at $T = 400$ K — about 30 K.

Experimental studies of the thermal conductivity of glassy crystals, ceramics and nanocomposites that have „gap" in the low-energy region of the phonon spectrum show that in this case, anomalies in the form of a local minimum or „plateau" are observed on the temperature dependence of the thermal conductivity coefficient [27–29]. A theoretical description of this effect was proposed in the paper [30], where it was shown that the location of „plateau" on the graph of the temperature dependence of thermal conductivity correlates with the position and width of *low-energy* (up to 10 K) „gap" in the phonon spectrum.

In our case, the „gap" is located in the middle region of the vibrational spectrum. As can be seen from the spectral density graph in Figure 1, b, at temperatures up to 200 K the number of zirconium phonons involved in energy transfer increases. At the same time, the interaction of phonons with each other increases, and accordingly, the curve k_p decreases. At $T = 200$ K a sharp decrease in the density of vibrational modes is observed. It is possible that from this moment the number of phonons involved in the transfer and dissipation of energy remains approximately at the same level. Accordingly, „plateau" is observed on the thermal conductivity curve. A further increase in temperature probably leads to the inclusion in the heat transfer process of optical phonons caused
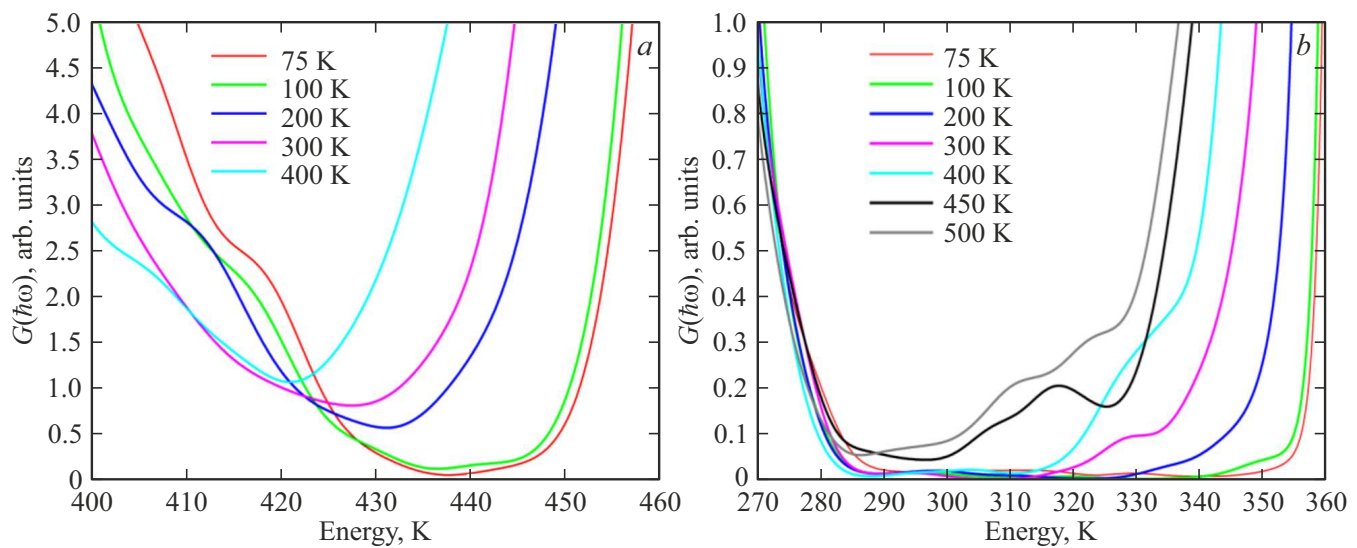
Figure 4. Vibrational density of states in region of „gap": (*a*) — Ti$_3$Al; (*b*) — Zr$_3$Al. Results are given for crystallites 48 u.c. long.

by vibrations of aluminum atoms, and increase in the interaction of phonons with each other. At that, thermal conductivity decreases in inverse proportion to temperature. It is worth noting that the Debye temperature (Θ_D), which characterizes the excitation energy of all possible phonons in the system under consideration, according to data [21,22] for Zr$_3$Al corresponds to $\Theta_D \sim 325$ K, which coincides with the „band gap" center. And in the vibrational spectrum of atoms Ti$_3$Al „gap" is very narrow and is located in a higher energy region, which corresponds to the temperature ~ 440 K.

Thus, it is possible that anomaly in the temperature dependence curve of lattice thermal conductivity may arise for compounds having such structure and interatomic interaction that would lead to the appearance of a wide „band gap" in the vibrational density of states. Moreover, this „gap" shall exist at temperatures above Θ_D. The presence of such conditions can apparently lead to the appearance of „step" or „plateau" in the temperature dependence curve of the lattice thermal conductivity. It is clear that this assumption requires more thorough verification, both theoretical and experimental. Preliminarily, we can say that test modeling of the Pt$_3$Al compound, in the L1$_2$ configuration, with potentials from the paper [30] shows that the vibrational density of states there is „band gap", which „collapses" when the temperature rises to 250 K. Accordingly, the curve $k_p(T)$ obtained for this compound on $12 \times 12 \times 48$ u.c. crystallite behaves similarly to that in compound Ti$_3$Al, no „plateau" is observed. To fully confirm or confute this assumption, it is necessary to find material, the vibrational spectrum of which has a sufficiently wide „band gap", that does not disappear until high temperatures (above Θ_D), and see how the values of lattice thermal conductivity coefficient will change with temperature.

5. Conclusion

In this paper the thermal properties of Ti$_3$Al and Zr$_3$Al intermetallides with the L1$_2$ structure were studied using the molecular dynamics method with interatomic interaction potentials made in the embedded atom model. The total and partial spectra of vibrational states and temperature dependences of heat capacities Ti$_3$Al and Zr$_3$Al, obtained during modeling were compared with the results of *ab initio* calculations. Both methods show that in both compounds the vibrational spectra of atoms are characterized by the band gap presence. In Zr$_3$Al the „gap" width is by order of magnitude greater than in Ti$_3$Al.

Calculations of lattice thermal conductivity based on the method of non-equilibrium molecular dynamics were carried out. The heat flow was simulated on crystallites with cross section 12×12 and lengths of 48 and 96 lattice cells along the direction of energy propagation. Graphs of the temperature dependence of the lattice thermal conductivity coefficient of structured intermetallides Ti$_3$Al and Zr$_3$Al were plotted. On the graphs $k_p(T)$ in Zr$_3$Al system in the temperature range 200 K $< T < 300$ K the lattice thermal conductivity coefficient practically does not change. It is assumed that this behavior $k_p(T)$ is associated with the „band gap" existence in the vibrational spectrum of atoms up to high temperatures (450 K $> \Theta_D$). In the compound Ti$_3$Al, where the phonon spectrum also has „band gap", but at temperature of 200 K it „collapses", and the lattice thermal conductivity decreases in inverse proportion to the temperature.

The presented model calculations of the thermal properties of Ti$_3$Al and Zr$_3$Al can be useful for the interpretation of future experiments and theoretical studies of processes in complex compounds where phonons play a significant role.

Funding

The paper was carried out using the cluster „Uran" of IMM SCC of Ural Branch of Russian Academy of Sciences within the framework of R&D topic of Udmurt Federal Research Center Ural Branch of the Russian Academy of Sciences „Theoretical studies of phase states, spectral and kinetic properties of electrons and phonons in systems with reduced dimension" No. 121030100005-1.

Conflict of interest

The authors declare that they have no conflict of interest.

Translated by I.Mazurov

References

[1] M. Maldovan. Phys. Rev. Lett. **110**, 025902 (2013).

[2] G. Wehmeyer, T. Yabuki, C. Monachon, J. Wu, C. Dames. Appl. Phys. Rev. **4**, 041304 (2017).

[3] T. Vasileiadis, J. Varghese, V. Babacic, J. Gomis-Bresco, D.N. Urrios, B. Graczykowski. J. Appl. Phys. **129**, 160901 (2021).

[4] P. Bhalla, P. Kumar, N. Das, N. Singh. Phys. Rev. B **94**, *11*, 115114 (2016).

[5] S. Cao, S. Xiao, Y. Chen, L. Xu, X. Wang, J. Han, Yi Jia. Mater. Des. **121**, 61 (2017).

[6] J. Chakraborty, K. Kumar, R. Ranjan, S. Ghosh Chowdhury, S.R. Singh. Acta Mater. **59**, *7*, 2615 (2011).

[7] X.Z. Ji, F. Jona, P.M. Marcus. Phys. Rev. B **68**, 075421 (2003).

[8] G.E. Hill, J. Marklund, J. Martinson, B.J. Hopkins. Surface Sci. **24**, *2*, 435 (1971).

[9] E.B. Dolgusheva, V.Yu. Trubitsin. Comp. Mater. Sci. **111**, 231 (2016).

[10] E.B. Dolgusheva. Comp. Mater. Sci. **155**, 55 (2018).

[11] E.B. Dolgusheva, V.Yu. Trubitsin. FTT **60**, *5*, 835 (2018). (in Russian).

[12] E.I. Salamatov, E.B. Dolgusheva. KhFM **23**, *4*, 486 (2021). (in Russian).

[13] E.B. Dolgusheva. KhFM **24**, *3*, 370 (2022). (in Russian).

[14] S.M. Foiles, M.I. Baskes, M.S. Daw. Phys. Rev. B **33**, 7983 (1986).

[15] H. Sheng. https://sites.google.com/site/eampotentials/Home/ZrAl

[16] R.R. Zope, Y. Mishin. Phys. Rev. B **68**, 024102 (2003).

[17] J.S.C. Jang, Y.W. Chen, L.J. Chang, H.Z. Cheng, C.C. Huang, C.Y. Tsau. Mater. Chem. Phys. **89**, 122 (2005).

[18] R. Tewari, G.K. Dey, S. Banerjee, N. Prabhu. Met. Mater. Trans. A **37**, 49 (2006).

[19] W.J. Meng, J.J. Faber, P.R. Okamoto, L.E. Rehn, B.J. Kestel, R.L. Hitterman. J. App. Phys. **67**, 1312 (1990).

[20] N. Arikan, M. Ersen, H.Y. Ocak, A. Iyigor, A. Candan, S. Ugur, G. Ugur, R. Khenata, D. Varshney. Mod. Phys. Lett. B **27**, *30*, 1350224 (2013).

[21] N. Arikan. J. Phys. Chem. Solids **74**, 794 (2013).

[22] H.L. Kagdada, H.J. Trivedi, S.B. Pillai, N.N. Som, P.K. Jha. AMR **1141**, 204 (2016).

[23] S. Plimpton. J. Comput. Phys. **117**, 1 (1995). http://lammps.sandia.gov

[24] P. Wirnsberger, D. Frenkel, C. Dellago. J. Chem. Phys. **143**, 124104 (2015).

[25] D.J. Evans, W.G. Hoover. Annu. Rev. Fluid Mech. **18**, 243 (1986).

[26] F. Müller-Plathe. J. Chem. Phys. **106**, **14**, 6082 (1997).

[27] R.G. Ross, P. Andersson, G. Backstrom. Nature **290**, 322 (1981).

[28] A.I. Krivchikov, B.Ya. Gorodilov, O.A. Korolyuk, V.G. Manzhelii, O.O. Romantsova, H. Conrad, W. Press, J.S. Tse, D.D. Klug. Phys. Rev. B **73**, 064203 (2006).

[29] A.I. Krivchikov, A.N. Yushchenko, O.A. Korolyuk, F.J. Bermejo, R. Fernandez-Perea, I. Bustinduy, M.A. González. Phys. Rev. B **77**, 024202 (2008).

[30] E. Salamatov. Chin. Phys. B **27**, *7*, 076502 (2018).

[31] J.S. Kim, D. Seol, J. Ji, H.S. Jang, Y. Kim, B.J. Lee. Calphad **59**, 131 (2017).